Functional Analysis of EBV in Nasopharyngeal Carcinoma Cells

Han-Chung Wu, Yu-Ju Lin, Jeng-Jie Lee, Yung-Jung Liu, Sung-Tzu Liang, Yet Peng, Yung-Wen Chiu, Chen-Wen Wu, and Chin-Tarng Lin

Department of Pathology (YP, C-TL), National Taiwan University Hospital, and Institute of Pathology (H-CW, Y-JL, J-JL, Y-JL, S-TL, YP, C-TL), College of Medicine, National Taiwan University, and National Health Research Institute (Y-WC, C-WW), Taipei, Taiwan

SUMMARY: A membrane invasion culture system was used to study the ability of EBV to enhance invasion and migration of nasopharyngeal carcinoma (NPC) cells. Semi-reverse transcriptase-PCR analysis of matrix proteinases and angiogenic factors from EBV-infected, or EBV-positive (EBV+), cells demonstrated different degrees of elevated gene expression. In our animal model, EBV+ tumors grew faster and larger than EBV-free, or EBV-negative (EBV−), tumors and also had clonal EBV terminal repeat sequences. Double-localization of EBV and certain host proteins in EBV+ tumors and biopsy specimens demonstrated that EBV up-regulates host genes only in cells that express those genes but not in cells that do not express them. Double-localization of EBV and host genes in NPC biopsy specimens all showed EBV− tumor cells expressing those host genes. Our data strongly suggest that EBV infection enhances progression of NPC tumor growth. They do not rule out a role for EBV infection in the induction and early promotion of NPC development. Unidentified factors may also enhance NPC tumor growth independent of the effects of EBV. (*Lab Invest 2003, 83:797–812*).

*E*BV has been closely associated with nasopharyngeal carcinoma (NPC), one of the most common cancers in South China, Taiwan, and Singapore (Klein et al, 1974; Niedobitek et al, 1991; Raab-Traub et al, 1983; Waterhouse et al, 1982). Heredity and environmental factors such as salted fish, Chinese herbs, and long-term exposure to sulfuric acid vapor may contribute to NPC induction (Armstrong et al, 1983; Ho et al, 1999).

To better understand the relationship between EBV and NPC, we have established nine NPC cell lines (Lin et al, 1990, 1993). Research findings regarding these cell lines and their original biopsy specimens can be summarized as follows (Lin et al, 1994, 1997a, 1997b, 2000): (a) Only five of nine lines contained the EBV genome, and all lines became EBV-negative (EBV−) after 30 passages (Lin et al, 1994); (b) In EBV-positive (EBV+) lines, only a fraction of tumor cells contained the episomal form of EBV DNA (Lin et al, 1994); (c) In situ hybridization and in situ PCR hybridization of original biopsy specimens demonstrated geographic distribution of EBV+ cells with a clonal expansion

growth pattern. EBV− cells were present in each case, and no untransformed squamous metaplastic epithelial cells contained the EBV genome (Lin et al, 1994); (d) EBV− cells can be infected through EBV-IgA-receptor secretory component (SC) protein–mediated endocytosis in vitro (Lin et al, 1997a); (e) Double-localization of EBV and SC demonstrated individual tumor cells containing both EBV and SC signals in the same biopsy specimen (Lin et al, 1997a); (f) Clonal EBV terminal repeat DNA sequences occur when NPC cells are infected by EBV in vitro (Lin et al, 1997b); (g) EBV infection can up-regulate expression of certain growth factors or cytokines (epidermal growth factor receptor [EGFR], transforming growth factor [TGF]-α, IL-1, IL-6, and granulocyte macrophage colony stimulating factor [GM-CSF]), but not of others (TGF-β1 and its receptors, IL-2, IL-4, IL-5, IL-8, and TNF-α) (Lin et al, 2000); and (h) Due to exocytosis of the EBV genome from host cells, most gene expression changes revert to original levels approximately 3 to 4 weeks after in vitro infection (Lin et al, 2000). These findings indicate that although EBV infection probably does not initiate NPC development, it can promote proliferation.

Miller et al (Miller et al, 1995) have demonstrated that EBV gene products such as LMP-1 up-regulate *EGFR* gene expression. All such research has used a single gene to investigate changes in expression of host genes. However, host cell response to a single transfected viral gene may differ from that to the whole viral genome. In the course of viral infection, there is no evidence to suggest that one virion affects the expression of only one gene. Therefore, to study the physiologic response to EBV infection, it is necessary

to infect cells in vitro and in vivo to obtain cellular reactions under normal physiologic conditions. Because an effective method to infect epithelial cells directly by EBV particles was not available in earlier research, study in this field has been limited. Our research is an in vitro and in vivo study that examines the effects of EBV infection on NPC progression. In vitro, we used receptor-mediated endocytosis (Lin et al, 1997a; Sixbey and Yao, 1992) to infect NPC cells and performed functional analysis to observe NPC invasiveness after EBV infection using membrane invasion culture system (MICS). In vivo, we transplanted EBV− NPC cells into severe combined immunodeficiency (SCID) mice. We then infected tumors with EBV. Growth- and invasion-related gene expressions were investigated in tumors and compared with biopsy specimens.

Results

Identification of EBNA-1 and EBV Genome in EBV+ NPC Cells

To confirm that EBV infection of NPC cells through IgA receptor-mediated endocytosis was feasible (Lin et al,

1994, 1997a) and to estimate infection efficiency, we used EBNA-1 antibodies to stain infected cells and used PCR Southern blotting and in situ PCR hybridization to localize the EBV genome in infected cells. PCR Southern blotting results showed a clear 110-bp band of EBV Bam H1 W fragments (data not shown). When EBV+ cells were fixed and stained with EBNA-1 antibody, anti–EBNA-1 reaction product was present in most tumor cells (Fig. 1A, arrows); a few cells had no reaction product (Fig. 1A, arrowhead). No reaction product was present in EBV− cells (Fig. 1B, arrow). Counting EBNA-1–positive cells from two EBV+ NPC cell lines in 20 high power fields (×400) yielded a 95% average infection rate. The in situ PCR hybridization study demonstrated a clear EBV DNA signal in most EBV+ cells (Fig. 1C, arrows); a few infected cells had no EBV DNA signal (Fig. 1C, arrowhead). No EBV− cell had an EBV DNA signal (Fig. 1D, arrow). Counting EBV DNA–positive cells from two EBV+ NPC cell lines in 20 high power fields (×400) yielded a 95% average infection rate. These findings are similar to those in our previous reports (Lin et al, 1994; Lin et al, 1997a; Lin et al, 2000).
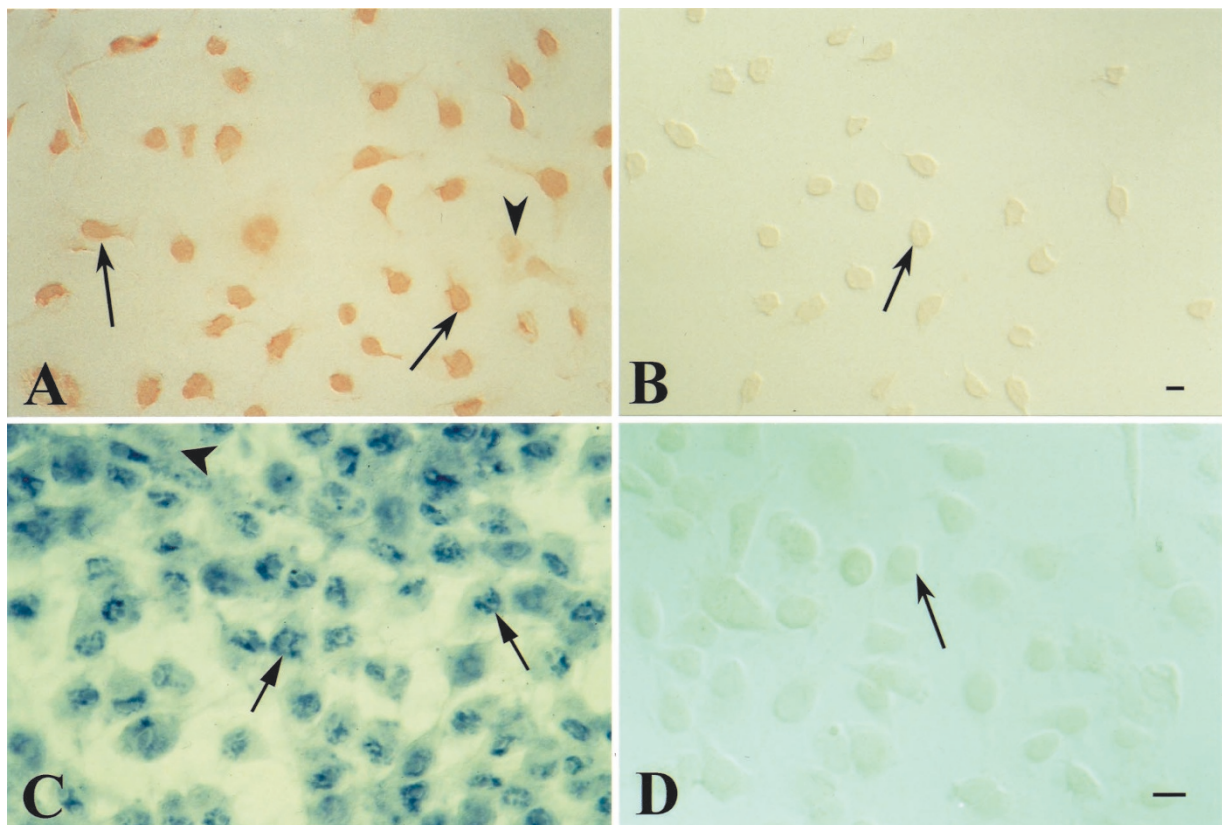
Figure 1.

Immunohistochemical localization of EBNA-1 and in situ PCR hybridization of EBV genome in EBV+ NPC-TW01 cell line. (A and C) Nasopharyngeal carcinoma (NPC) cells treated with IgA anti-EBV-VCA + EBV particles; (B and D) NPC cells only treated with EBV particles. (A and B) Immunostained by mAb against EBNA-1; (C and D) NPC cells were fixed for in situ PCR first, followed by in situ hybridization with dig-labeled EBV (BamH1 DNA) probe. (A) Most NPC cells show immunoreactivity of anti-EBNA-1 in their nuclei (*arrows*). A few are unstained (*arrowhead*). (B) No immunoreactivity of anti-EBNA-1 is shown (*arrow*). (C) EBV DNA signal is also seen in most NPC culture cells (*arrows* indicate EBV-signal positive cells; *arrowhead* indicates EBV-signal negative cells). (D) No EBV DNA signal (*arrow*) is seen in any tumor cell. The average percentage of EBV+ cells is 95%, a figure obtained by counting the number of EBV+ cells in 20 fields at ×400 magnification from A and C. Bar in A and B = 20 μm; bar in C and D = 20 μm.

### Membrane Invasion Culture Assay for EBV+ NPC Cells

Membrane invasion culture assay was used to analyze invasive activity of EBV+ cells. We cultured EBV+ and EBV− cells in matrigel-coated membranes and incubated them for 7, 14, and 21 days. Number of invaded cells after 7 days was 1.4 times higher in EBV+ cultures than in EBV− controls. After 14 days, the number of invaded cells increased to 2.5 times higher than in controls. After 21 days, the number of invaded cells decreased to 1.4 times the control level (Fig. 2).

Semi-Quantitative RT-PCR Analysis of Invasion-Related Gene Expression in EBV+ NPC Cells
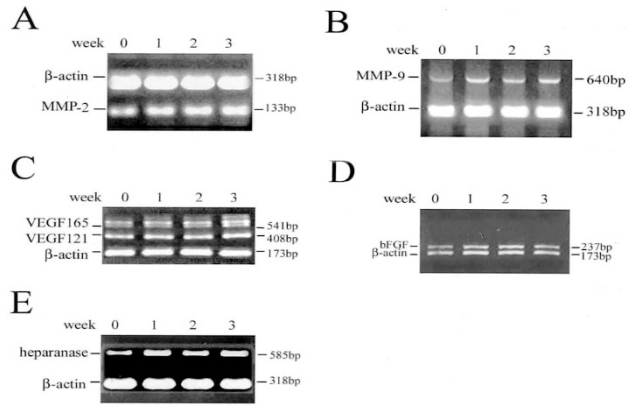
To observe invasion-related gene expression in EBV+ host cells, we investigated gene expressions of three matrix proteases and two angiogenic factors. When total RNA was isolated from EBV+ cells after incubation for 0, 7, 14, and 21 days and then subjected to RT-PCR analysis, we found that matrix metalloproteinase (MMP)-2 gene expression had been moderately up-regulated and was time dependent (Fig. 3A). MMP-9 and heparanase also had moderate gene expression up-regulation, but their elevations were variable at different time intervals (Fig. 3, B and E). When we analyzed vascular endothelial growth factor (VEGF) and basic fibroblast growth factor (bFGF) RNA, we found that VEGF gene expression was mildly up-regulated (Fig. 3C). bFGF expression was unchanged (Fig. 3D). Densitometry analysis of RT-PCR data (Fig. 4) showed that (a) MMP-2, MMP-9, and heparanase were moderately up-regulated and were either time dependent or showed variable elevations at different times; (b) VEGF (121 bp was used as the representative band) was mildly up-regulated; and (c) bFGF showed no significant change.

### Growth, Morphological Changes, and EBV Genome Observations in EBV+ and EBV− tumors

To investigate the behavior of EBV+ cells in vivo, we implanted EBV− NPC cells into SCID mice and sub-
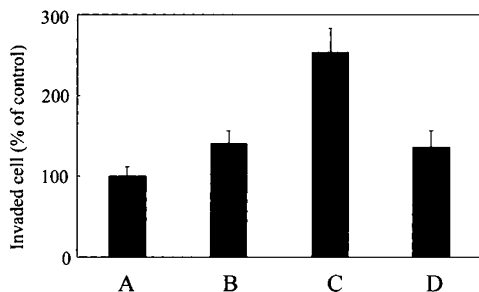
Figure 2.
Analysis of invasive ability of nasopharyngeal carcinoma cells using MICS. The invasive abilities of cells were measured in vitro with the membrane invasion culture system chamber as described in Materials and Methods. NPC-TW01 cells (2.5×10^3) after EBV infection in vitro were seeded on Matrigel, and invaded cells were examined after 48 hours. EBV+ cells were incubated for 0 day (A), 1 week (B), 2 weeks (C), and 3 weeks (D). *Bar graphs* represent average % of invasiveness compared with control cells + standard error: A = 100 ± 11.5%; B = 140 ± 13.7%; C = 254 ± 19.7%; and D = 136 ± 17.2%.

Figure 3.
Semi-quantitative RT-PCR analysis of invasion-related host gene expressions in EBV+ NPC cells. After EBV infection in the in vitro culture system as mentioned in Figure 1, NPC cells were cultured for 1, 2, and 3 weeks and harvested for total RNA extraction for RT-PCR analysis. (A) MMP-2, (B) MMP-9, (C) VEGF, (D) bFGF, and (E) heparanase. The 133-bp MMP-2 band, the 640-bp MMP-9 band, and the 585-bp heparanase band show increased intensity ($> \times 2.5$) when incubation time was increased from 0 weeks to 3 weeks. After incubation for 3 weeks, intensities of the 165- and 121-bp VEGF bands only slightly increased ($> \times 2.5$) and of the 237-bp bFGF band showed no remarkable change.
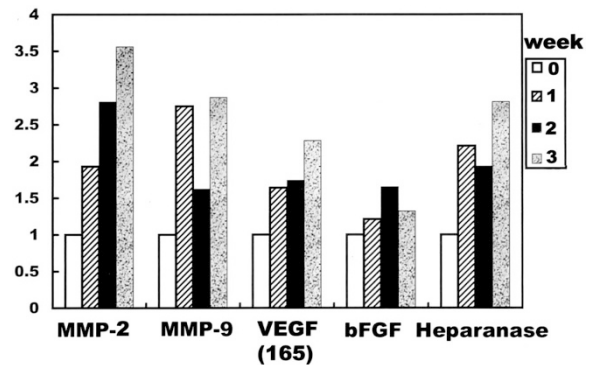
Figure 4.
Densitometry analysis of EBV-related host gene expressions. Data were obtained from gel electrophoresis analysis in Figure 3. Each gene expression shows four different bars. From left to right, they represent the different EBV-infection periods of 0, 1, 2, and 3 weeks, respectively. Matrix metalloproteinase (MMP)-1, MMP-9, and heparanase show moderate gene expression elevation ($> \times 2.5$) after EBV infection and incubation for 3 weeks. *VEGF* gene was mildly up-regulated ($\times 1.5$ to $\times 2.5$). bFGF was minimally changed ($< \times 1.5$).

sequently injected IgA anti-EBV-VCA and EBV particles into solid tumor nodules. Three weeks later, tumors that had been injected with IgA anti-EBV-VCA and EBV particles had grown faster and larger (average tumor volume [TV] = 1.56 cm^3) than EBV-free tumor masses, including those injected with EBV only (TV = 0.86 cm^3) or those without injection of any kind (TV = 0.90 cm^3) (Table 2). TV was calculated using the formula: TV = L × W^2 × 0.5. (L and W represent tumor length and width, respectively.)

Hematoxylin and eosin staining of EBV+ and EBV− tumor sections from the NPC-TW01 line showed keratinizing squamous cell carcinoma with areas of nonkeratinizing undifferentiated tumor cells (data not shown). Mitotic and apoptotic cells were seen more

Table 1. Oligonucleotide Primer Sequences Used for RT-PCR

Primer	Sequence[a]	Size (bp)	Reference
MMP-2	F-GGGGCCTCTCCTGACATT	133	Nuovo et al, 1995
	E-TCACAGTCCTGACATT		
MMP-9	L-GGTCCCCCCACTGCTGGCCCTTCTACGGCC	64	Morgan et al, 1998
	R-GTCCTCAGGGCACTGCAGGATGTCATAGGT		
Heparanase	TTCGATCCCAAGAAGGAATCAAC	585	Vlodavsky et al, 1999
	GTAGTGATGCCATGTAACTGAATC		
VEGF	GAAGTGGTGAAGTTCATGGATGTC	541, 408	Ohta et al, 1996
	CGATCGTTCTGTATCAGTCTTTCC		
bFGF	GTGTGTGCTAACCGTTACCT	237	Ohta et al, 1996
	GCTCTTAGCAGACATTGGAAG		

bFGF, basic fibroblast growth factor; MMP, matrix metalloproteinase; VEGF, vascular endothelial growth factor.
[a] All the primers' sequences were adapted from published reports in the Reference column. The primers for epidermal growth factor receptor, TGF-α, TGF-$\beta1$, TGF-βR1 TGF-βRII, secretory component, and the internal control GAPDH and actin sequences were used as in our previous report (Lin et al, 2000).

Table 2. Growth Patterns in Animal Models Bearing with EBV-Infected and -Free NPC Cells[a]

	Treatment			EBV evaluation	
	IgA anti-EBV	EBV	Tumor size[e] (cm³)	PCR Southern blotting	EBER-1 in situ hybridization
I[b]					
1	−	+	0.73	−	−
2	−	+	0.98	−	−
Average			0.86		
II[c]					
1	+	+	1.95	−	+
2	+	+	1.56	+	+
3	+	+	1.21	+	−
4	+	+	1.50	−	+
5	+	+	1.56	+	+
Average			1.56		
III[d]					
1	−	−	0.60	−	−
2	−	−	1.08	−	−
3	−	−	1.01	−	−
Average			0.90		

[a] EBV-free NPC-TW01 cells (1 × 10⁷) were injected into 10 SCID mice. Seven days later, five mice were injected with IgA anti-EBV and EBV particles, separately, two with EBV particles only, directly into the solid tumor masses; another three were kept without any treatment. The tumor masses were dissected after another 3 weeks.
[b] Solid tumors injected with EBV particles only. Animals were killed at 28th day after they were injected with tumor cells.
[c] Solid tumors injected with IgA anti-EBV + EBV particles. All animals were killed at 28th day after they were injected with tumor cells.
[d] Solid tumors without any treatment. All animals were killed at 28th day after they were injected with tumor cells.
[e] Tumor size was calculated by length × (width)² × 0.5.

often in EBV+ and less often in EBV− tumor sections. In EBV+ tumor sections, average numbers of mitotic cells and apoptotic cells were 9 and 13 cells per high power field (×400), respectively. In EBV− tumor sections, average numbers of mitotic cells and apoptotic cells were 7 and 12.8 cells per high power field, respectively. Averages were obtained from 20 high power field counts. When total DNA was extracted from randomly selected fragments of each EBV+ tumor, some had a 110-bp band of EBV DNA in *Bam*HI fragments by PCR Southern blotting, similar to in vitro observations. Tissue fragments from other tumors had no EBV signal (Table 2). If in situ hybridization was used to identify EBER-1 in tumor cells, some tissue fragments were positive for EBV, while others were negative (Table 2). Nevertheless, all were positive for EBV by either PCR Southern blotting or in situ hybridization, or by both (Table 2). Different EBV+ or EBV− results in tissue fragments were mainly due to the EBV infection method used in which both IgA anti-EBV-VCA and EBV particles were injected separately and directly into solid tumor masses. Distributions of

EBV+ and EBV− tumor cells were different in each tumor mass in in situ hybridization. EBV+ cells were seen mostly surrounding the injected site (Fig. 5, A and C). Many EBV+ cells were intermixed with EBV− cells and showed clonal proliferation (Fig. 5B, between two arrows). In some tumor nests, the central differentiated region contained fewer EBV+ cells (Fig. 5D, small arrows). Some EBV+ (Fig. 5D, large arrowhead) and EBV− (Fig. 5D, large arrow) differentiated tumor cells also showed apoptotic change. If tumor was injected with EBV only, without IgA anti-EBV, no EBV signal was present (Fig. 8B).

Identification of Clonal EBV Terminal Sequence Repeats in EBV+ Solid Tumor Masses

To see if the in vitro finding that EBV+ NPC cells had a clonal EBV genomic DNA sequence (11) was present in the in vivo animal model, we examined solid tumor masses removed from two SCID mice that had been injected with NPC-TW01 and 06 cells and infected by EBV (IgA anti-EBV-VCA + EBV). We subjected tumors to total DNA isolation. For comparison, we examined tumors obtained from a SCID mouse that had been injected with NPC cells and EBV only (without IgA). In addition, total DNA isolated from the Raji and the B95−8 cell lines were also examined. All DNA samples were analyzed by Southern blotting using a ^{32}P-labeled *Xho*I 1.9 kb DNA fragment probe (Lin et al, 1997b). B95−8 cells had multiple bands of terminal repeats and a major 18- to 30-kb band (Fig. 6, lane 2). Raji cells had a single 23-kb band (Fig. 6, lane 1). Two EBV+ tumors also showed a single band but of a different size (Fig. 6, lane 3 [NPC-TW 01 line] and lane 4 [NPC-TW 06 line]). The tumors from the SCID mouse that had been injected with NPC cells and EBV particles only (without IgA) had no EBV band (Fig. 6, lane 5). The major 18- to 30-kb band in the B95−8 line probably corresponds to the major 15- to 20-kb band in well-separated gel (Figs. 2 and 3 in Lin et al, 1997b revealed two well-separated gels and showed the same major 15- to 20-kd band). This band may be derived from fused termini bands.

Host Gene Expressions Changes in EBV+ Tumors

Because EBV+ tumors grew faster and larger than EBV− tumors, we examined expression of growth
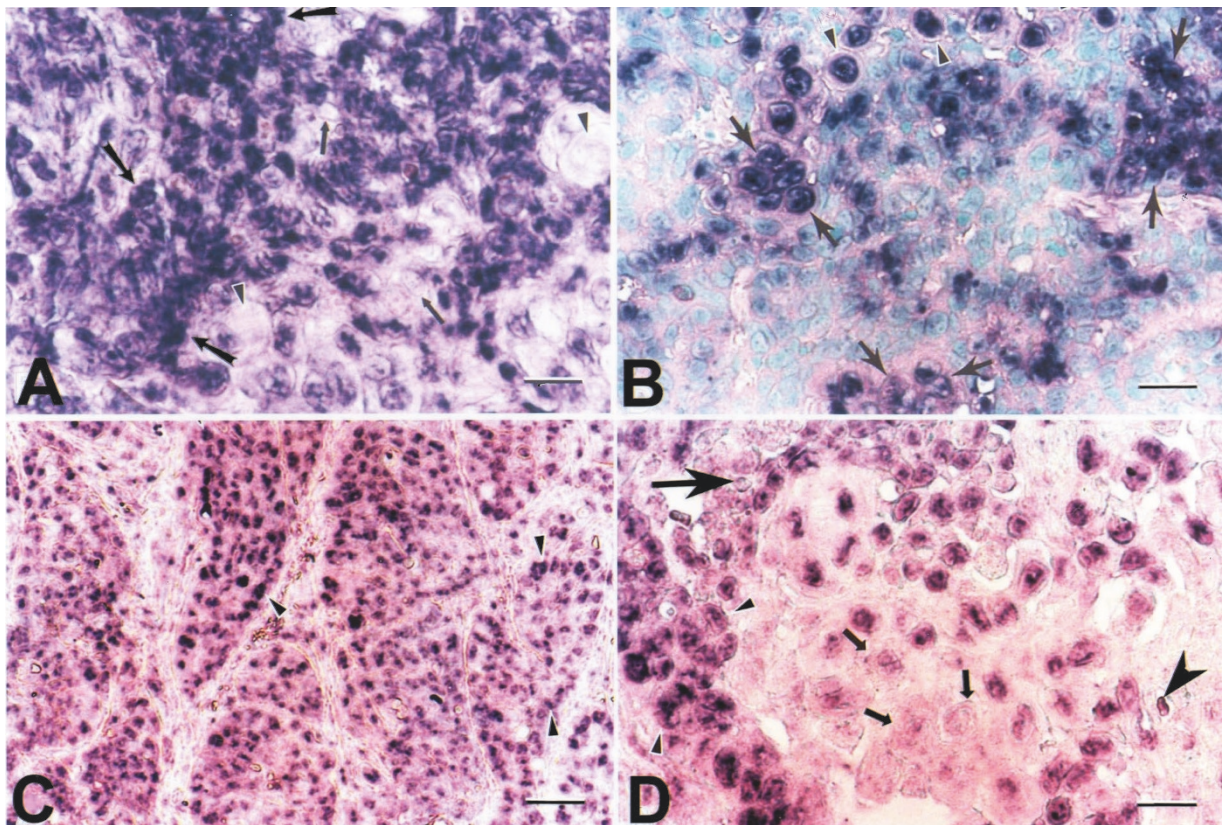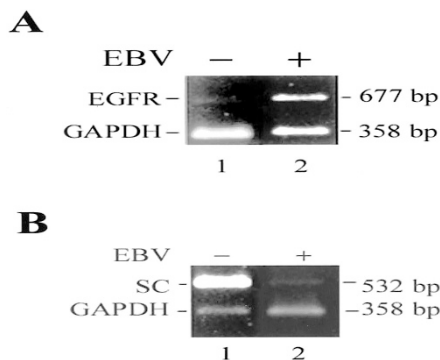

Figure 5.

In situ nucleic acid hybridization of EBV encoded small nuclear RNA-1 (EBER-1) in EBV+ tumors obtained from SCID mice. The pictures were taken from four different tumor sections. (A) EBV+ cells aggregated in areas surrounding the injected site (between *large arrows*). EBV+ cells invade the surrounding EBV− region (*small arrows*). A few differentiated cells (*arrowheads*) showing no EBV signal are discernible. (B) At the junctional zone between EBV+ and EBV− cells, some EBV+ cells are invading the EBV− region. Sometimes these invading cells proliferated and aggregated to form tumor nests (between *arrows*) consistent with clonal expansion. EBV+ cells, which did not form tumor nests, are also present (*arrowheads*). (C) EBV+ cells in aggregated nests (*arrowheads*) surrounded by stromal tissue. (D) Higher magnification demonstrates prominent EBV+ cells (between *small arrowheads*) at the periphery of a tumor nest. The intensity of the EBV signal is decreased in the more differentiated cells in the tumor nest center (*small arrows*). Apoptotic changes are present in some EBV+ (*large arrowhead*) and EBV− tumor cells (*large arrow*). Bar in A, B, and D = 28 μm; bar in C = 52 μm.
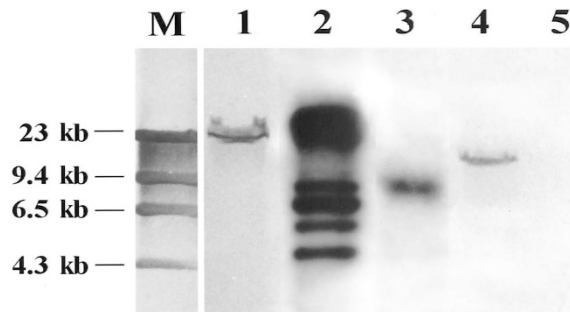
Figure 6.

Southern blot analysis of EBV terminal repeat pattern in EBV+ nasopharyngeal carcinoma (NPC) tumors: lane 1, Raji cell; lane 2, B95–8 cell line; lane 3, in vivo EBV+ NPC TW01 tumor; lane 4, in vivo EBV+ NPC-TW06 tumor; and lane 5, an EBV− solid tumor produced by injection of NPC-TW01 cells. Except for lane 2, which has one major 18- to 30-kb band (probably derived from fused termini bands) and other multiple bands, lanes 1, 3, and 4 each has a homogeneous single band of terminal repeat EBV DNA sequences of different sizes. Lane 5 shows no EBV genome. M is a size marker.

factor related genes. EGFR and TGF-α gene expressions were increased in EBV+ tumors. A representative gel analysis is shown in Figure 7A. TGF-β1, TGF-β receptor-I, and TGF-β receptor-II gene expressions were not significantly different in EBV+ and EBV− tumors (data not shown). In our previous report (Lin et al, 1997a), we presented data indicating that in vitro EBV infection can suppress SC protein. We wanted to know whether this phenomenon occurred in our animal model. RT-PCR analysis of SC-mRNA expression demonstrated marked down-regulation of SC gene expression in EBV+ tumors (Fig. 7B), similar to our previous in vitro experiment (Lin et al, 1997a). To confirm the presence of overexpressed EGFR and underexpressed SC mRNA, we used antibodies against EGFR and SC to stain tumor sections. Enhancement of EGFR immunostaining was clearly evident in EBV+ tumors. Many cells had a strong staining reaction, and a small number had no staining reaction (Fig. 8A). When antibodies against SC protein were used, SC immunostaining was almost invisible in EBV+ tumor sections (data not shown).

Figure 7.

Semi-quantitative RT-PCR analysis of epidermal growth factor receptor (EGFR) and secretory component (SC) protein mRNA expression. EBV+ and EBV− tumors dissected from SCID mice were subjected to total RNA extraction for RT-PCR analysis. Lane 1, from an EBV− NPC tumor; lane 2, from an EBV+ tumor. (A) An increase in EGFR mRNA expression is shown in the EBV+ tumor (lane 2) when compared with the EBV− tumor (lane 1). Glyceraldehyde phosphate dehydrogenase is the internal control. (B) Marked decrease in SC mRNA expression is shown in EBV+ tumors (lane 2) when compared with the EBV− tumors (lane 1).

Co-Localization of EBV and Host Gene Expressions in Solid Tumors from SCID Mice

To investigate the relationship of the EBV genome with growth and invasion related gene expressions in EBV+ cells in solid tumors, we performed double-localizations of host proteins and EBER-1. In EBV+ tumor sections, many cells tested positive for EBV, and only a fraction were strongly EGFR immunoreactive (Fig. 8A, arrowhead). Many EBV+ cells showed no EGFR immunoreactivity (Fig. 8A, arrow). In EBV− tumor sections, only certain cells had moderate EGFR immunoreactivity (Fig. 8B, large arrowhead), and other cells had no EGFR staining (Fig. 8B, small arrowhead). In situ hybridization of EBER-1 in the same EBV− sections showed no EBV signal (Fig. 8B).

When MMP-2 and EBER-1 were co-localized in EBV+ sections, most cells showed no or nonspecific background staining (Fig. 8C, black arrowhead); only a few clearly had immunostaining (Fig. 8C, large white arrowhead). However, many interstitial mesenchymal cells were strongly immunoreactive (Fig. 8C, arrow). In EBV− tumor sections, only a few tumor cells were immunostained (Fig. 8D, arrows) and most were stain-free (Fig. 8D, small arrowhead). Many interstitial mesenchymal cells also contained anti–MMP-2 immunostaining (Fig. 8D, large arrowhead).

In the case of MMP-9, many EBV+ cells had strong anti–MMP-9 immunostaining (Fig. 8E, arrow), but others did not (Fig. 8E, arrowhead). Similarly, in EBV− tumor sections, many cells had anti–MMP-9 immunostaining (Fig. 8F, arrow), but others did not (Fig. 8F, arrowheads). These finding are similar to those with regard to EGFR expression in EBV+ and EBV− tumor sections. Interstitial mesenchymal cells in both sections were rarely stained (Fig. 8, E and F).

With regard to VEGF co-localization, many EBV+ cells were anti-VEGF immunoreactive (Fig. 9A, arrowheads), and a few were not (Fig. 9A, single arrows). Immunoreactivity was also seen on or in vascular walls and in endothelial cells (Fig. 9A, double arrows). In EBV− sections, anti-VEGF immunoreactivity was also seen in some tumor (Fig. 9B, large arrowhead) and
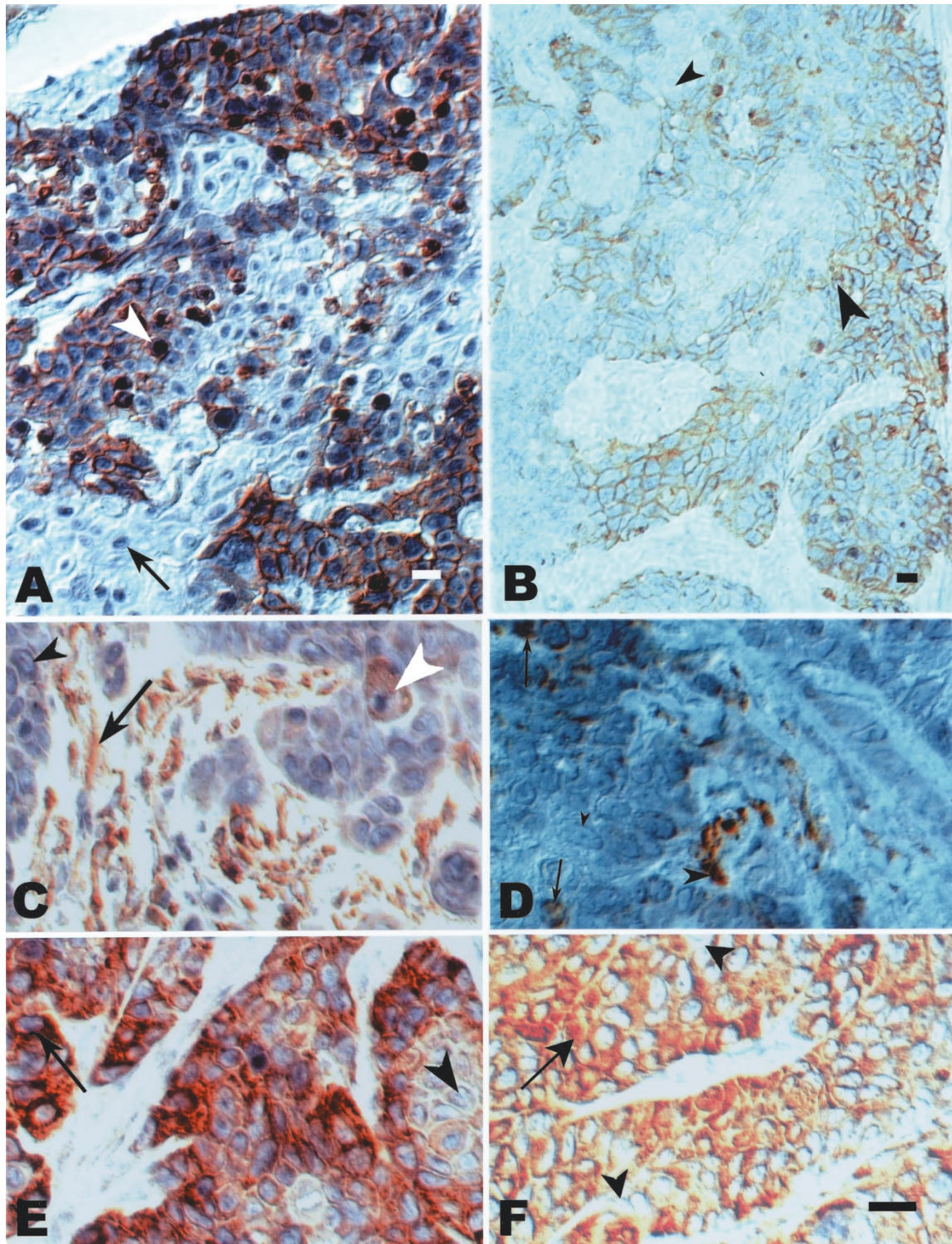
Figure 8.

Co-localization of epidermal growth factor receptor (EGFR), MMP-2, and matrix metalloproteinase (MMP)-9 with EBER-1, separately, in EBV+ and EBV− tumors obtained from SCID mice. (A, C, and E) EBV+ tumor sections. (B, D, and F) EBV− tumor sections. EBV signal is blue to purple in color and is localized in the nuclei of most tumor cells; brown reaction indicates each host gene product. (A and B) Co-localization of EGFR and EBER-1. (A) Most tumor cells show clear EBER-1 signals (*arrow*), but only a fraction also contain strong EGFR immunoreactivity (*large white arrowhead*). (B) No EBV signal is shown in the EBV− section, but EGFR immunoreactivity is seen in certain tumor cells (*large black arrowhead*); another group of tumor cells contain no EGFR reaction product (*small black arrowhead*). (C and D) Co-localization of MMP-2 and EBER-1. (C) Anti–MMP-2 reaction product is shown in a few EBV+ NPC cells (*large white arrowhead*) and strong reaction product is also seen in stromal mesenchymal cells (*black arrow*). However, many tumor cells containing EBER-1 signal with background cytoplasmic staining but no MMP-2 reaction product (*black arrowhead*) are shown. (D) The EBV− section shows MMP-2 reaction product in some tumor cells (*arrows*). Most tumor cells (*small arrowhead*) do not have MMP-2 immunoreactivity; however, some mesenchymal cells are strongly immunoreactive (*large black arrowhead*). (E and F) Co-localization of MMP-9 and EBER-1. (E) In EBV+ tumor sections, there is strong anti-MMP-9 immunoreactivity (*arrow*). Some MMP-9-negative EBV+ cells are also identified (*arrowhead*). Interstitial cells rarely show MMP-9 reactivity. (F) In EBV− tumor sections, many tumor cells are anti–MMP-9 immunoreactive (*arrow*). Some are not reactive (*arrowheads*). Interstitial cells show no reaction.
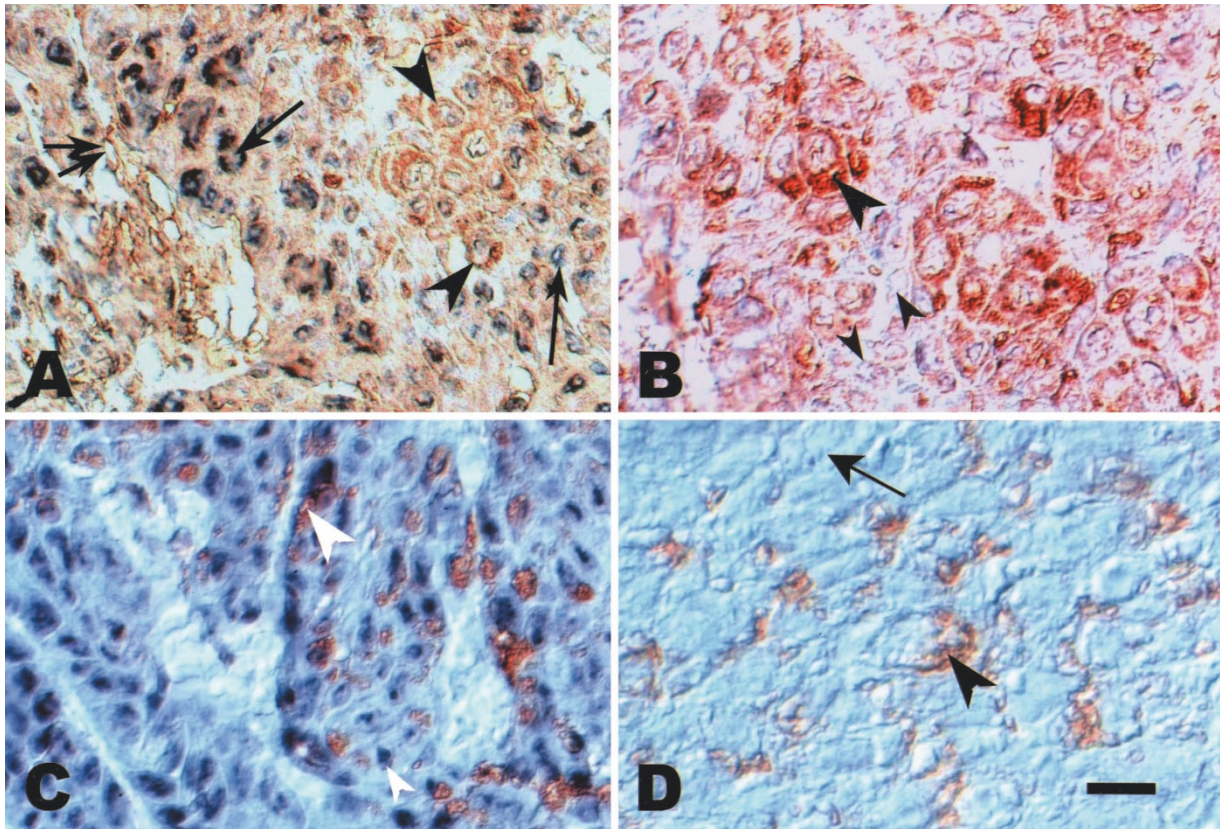
Figure 9.
Co-localization of vascular endothelial growth factor (VEGF) and basic fibroblast growth factor (bFGF) proteins with EBER-1, separately, in EBV+ and EBV− severe combined immunodeficiency (SCID) tumors. (A and C) EBV+ tumor sections. (B and D) EBV− tumor sections. (A and B) Tumor sections were immunostained with anti-VEGF and in situ hybridized by EBER-1 antisense probe. (C and D) Sections were immunostained with anti-bFGF and in situ hybridized with EBER-1 probe. (A) Most tumor cells show EBER-1 signal in their nuclei (dark blue). Some have cytoplasmic immunostaining of anti-VEGF (*arrowheads*, yellowish brown). Other tumor cells have nonspecific background EBER-1 signal staining (*large arrows*). Anti-VEGF reactivity is seen in endothelial cells (*double small arrows*). (B) Many tumor cells (*large arrowhead*) are VEGF immunoreactive. A few are nonreactive (*small arrowhead*). No EBER-1 signal is seen in any tumor cells. (C) Only a fraction of tumor cells (*large white arrowhead*) contains an EBV signal and is bFGF immunoreactive. Many cells show EBV signal only (*small white arrowhead*). (D) Some tumor cells (*arrowhead*) contain bFGF reaction product, but most do not (*arrow*). Bar in D for A, B, C, and D = 28 μm.

endothelial cells. Some tumor cells had no or very weak staining (Fig. 9B, small arrowhead).

In the case of bFGF, only some EBV+ cells contained bFGF immunoreactivity (Fig. 9C, large white arrowhead); many others were free of bFGF immunostaining (Fig. 9C, small white arrowhead). In EBV− sections, only certain tumor cells contained bFGF reaction product (Fig. 9D, arrowhead), a finding similar to that in EBV+ sections; all tumor cells were EBV− (Fig. 9D, arrow). The average numbers of EBV+ cells and cells containing each antiprotein reaction product are shown in Tables 3 to 7. They were obtained by counting 15 high power fields (×400) in all double-localization sections.

Western Blot Analysis of EGFR Protein Expression in EBV+ Tumors

Although different staining intensities could easily be identified in EGFR immunohistochemical localizations in EBV+ sections, it was difficult to quantify levels of EGFR expression. Therefore, we used routine Western blot analysis to examine EGFR expression levels. We

found that EGFR protein expression in EBV+ cells was 1.7-fold higher than in EBV− cells. (Fig. 10).

Co-Localization of EBV and Host Gene Expressions in NPC Biopsy Specimens

To confirm observations from xenograft tumor masses dissected from SCID mice, we collected 20 NPC primary biopsy specimens that had been examined by PCR and Southern blotting previously and that had tested positive for EBV infection. Paraffin block sections were then examined.

After performing in situ hybridization using EBER-1 antisense probe, we found that all NPC specimens had some EBV+ and EBV− tumor cells (Fig. 11, B to F). When sections were examined by in situ PCR hybridization, similarly some EBV+ cells (Fig. 11A, arrows) and EBV− cells (Fig. 11A, large and small arrowheads) were also found. Both methods had produced similar results. In some cases, sections contained more EBV+ cells and in others more EBV− cells. Average EBV+ cell numbers in 20 biopsy specimens by in situ hybridization and in situ

Table 3. Co-Localization of EGFR and EBER-1

Nasopharyngeal carcinoma (NPC)						
Human cases	1	2	3	4	5	Average[a] (%) +
EGFR	38	40	56	53	44	46
EBER-1	64	67	71	89	67	72
EGFR + EBER-1	25	26	42	47	36	35

Mouse tumor		
Mouse tumor masses	EBV-infected[b] (%) +	EBV-free (%) +
EGFR	73	75
EBER-1	98	0
EGFR + EBER-1	67	0

EGFR, epidermal growth factor receptor.

In each case, the stained cell number was obtained from the average of 15 high power field counts (×400).

[a] The average percentage was obtained from five biopsy specimens.

[b] In each case, the percentage of stained cell number was obtained from the average of counting 20 high power fields (×400).

Table 4. Co-Localization of MMP-2 and EBER-1

NPC			
Human cases[a]	1	2	3	Average[b] (%) +
MMP-2	38	4	7	16
EBER-1	91	80	76	82
MMP-2 + EBER-1	36	1	2	13

Mouse tumor		
Mouse tumor masses	EBV-infected[c] (%) +	EBV-free (%) +
MMP-2	27	30
EBER-1	98	0
MMP-2 + EBER-1	27	0

MMP, matrix metalloproteinase; NPC, nasopharyngeal carcinoma.

[a] In each case, the percentage of stained cell number was obtained from the average of counting 15 high power fields (×400).

[b] The average percentage was obtained from three NPC biopsy specimens.

[c] In each case, the percentage of stained cell number was obtained from the average of counting 20 high power fields (×400).

Table 5. Co-Localization of MMP-9 and EBER-1

NPC			
Human cases[a]	1	2	3	Average[b] (%) +
MMP-9	60	49	47	52
EBER-1	74	64	79	72
MMP-9 + EBER-1	42	40	38	40

Mouse tumor		
Mouse tumor masses	EBV-infected[c] (%) +	EBV-free (%) +
MMP-9	87	92
EBER-1	98	0
MMP-9 + EBER-1	82	0

MMP, matrix metalloproteinase.

[a] In each case, the percentage of stained cell number was obtained from the average of counting 15 high power fields (×400).

[b] The average percentage was obtained from three biopsy specimens.

[c] In each case, the percentage of positive stained number was obtained from the average of counting 20 high power fields (×400).

Table 6. Co-Localization of VEGF and EBER-1

NPC		
Human cases[a]	1	2	Average[b] (%) +
VEGF	57	70	64
EBER-1	55	46	51
VEGF + EBER-1	40	42	41

Mouse tumor		
Mouse tumor masses[c]	EBV-infected (%) +	EBV-free (%) +
VEGF	70	75
EBER-1	95	0
VEGF + EBER-1	65	0

NPC, nasopharyngeal carcinoma; VEGF, vascular endothelial growth factor.

[a] In each case, the percentage of stained cell number was obtained from the average of counting 15 high power fields (×400).

[b] The average of percentage was obtained from two NPC biopsy specimens.

[c] In each case, the average of stained cell number was obtained from the average of 20 high power field counts (×400).

PCR hybridization methods were similar and ranged between 72% and 82%. These data were obtained by averaging EBV+ cell numbers in each of 20 cases. EBV+ cell numbers were obtained from 15 high power field (×400) counts. Two to five representative NPC cases (WHO Type I, keratinizing squamous cell carcinoma or WHO Type IIb, undifferentiated carcinoma) were used for co-localization of EBV with EGFR, matrix proteinases, and angiogenic factors. When NPC biopsy specimens were co-localized with EBER-1 and EGFR protein, some EBV+ cells contained EGFR immunoreactivity (Fig. 11B, large white arrowhead), while others did not (Fig. 11B, small white arrowhead). In EBV− cells (Fig. 11B, small black arrowhead), there were instances of EGFR immunostaining (Fig. 11B, large black arrowhead).

If biopsy sections were stained with MMP-2 and EBER-1, only a small fraction of cells showed the EBER-1 signal (Fig. 11C, white arrowhead). EBV+ cells very rarely expressed MMP-2. Very few EBV− tumor cells (Fig. 11C, small black arrowhead) contained MMP-2 reaction product (Fig. 11C, large black

Table 7. Co-Localization of bFGF and EBER-1

Human cases[a]	1	2	3	Average[b] (%) +
bFGF	39	20	33	31
EBER-1	72	59	51	61
bFGF + EBER-1	27	17	20	21

Mouse tumor masses[c]	EBV-infected (%) +	EBV-free (%) +
bFGF	32	35
EBER-1	96	0
bFGF + EBER-1	29	0

bFGF, basic fibroblast growth factor; NPC, nasopharyngeal carcinoma.

[a] In each case, the average of stained cell number was obtained from the average of counting 15 high power fields (×400).

[b] The average of percentage was obtained from three NPC biopsy specimens.

[c] In each case, the average of stained cell number was obtained from the average of counting 20 high power fields (×400).

arrowheads). However, some interstitial mesenchymal cells demonstrated MMP-2 reaction product.

In the case of MMP-9, certain EBV+ and EBV− tumor cells showed MMP-9 immunoreactivity (Fig. 11D, short arrow; and Fig. 11D, inset black arrowhead), but anti–MMP-9 immunoreactivity was also seen in interstitial mesenchymal and mononuclear cells (Fig. 11D, long arrows). Some EBV+ tumor cells showed no MMP-9 immunoreactivity (Fig. 11D, small arrowhead).

When VEGF antibodies and in situ hybridization of EBER-1 were applied to NPC specimens, VEGF immunoreactivity was seen in EBV+ cells (Fig. 11E, arrow) and in certain EBV− cells (Fig. 11E, large black arrowhead). Furthermore, a fraction of tumor cells were EBV− and VEGF-negative (Fig. 11E, small black arrowhead).

When anti-bFGF and in situ hybridization of EBER-1 were applied to NPC specimens, some cells were bFGF reactive (Fig. 11F, large black and large white arrowheads). Only some of these bFGF reactive cells contained the EBV signal (Fig. 11F, large white arrowhead). Many bFGF unreactive cells had the EBV signal (Fig. 11F, small white arrowhead). However, certain tumor cells were neither EBV-DNA nor bFGF immunoreactive (Fig. 11F, small black arrowhead).

Average numbers of EBV+ cells and cells containing specific proteins in biopsy specimens are shown in Tables 3 to 7. Because antibodies for heparanase were not available, we did not perform immunostaining for heparanase.

Discussion

Patients who have undifferentiated NPC usually have high titers of IgA anti-EBV-VCA, especially if the tumor is infected by EBV. In many cases, EBV+ tumors have
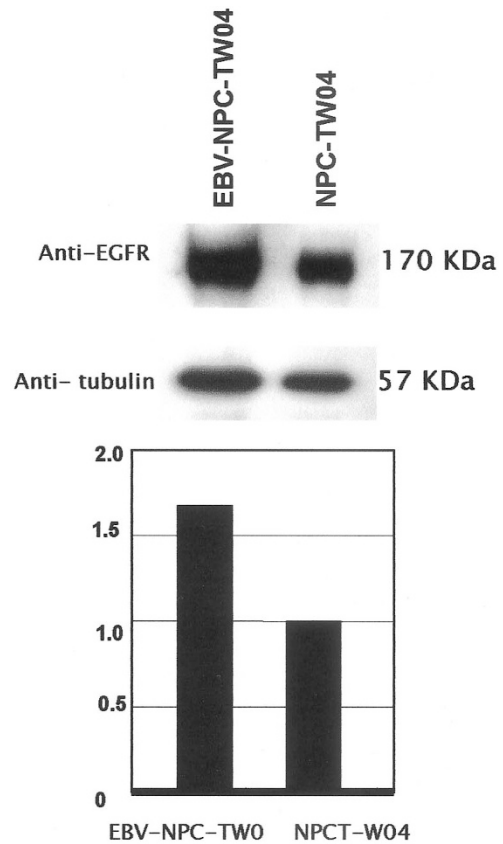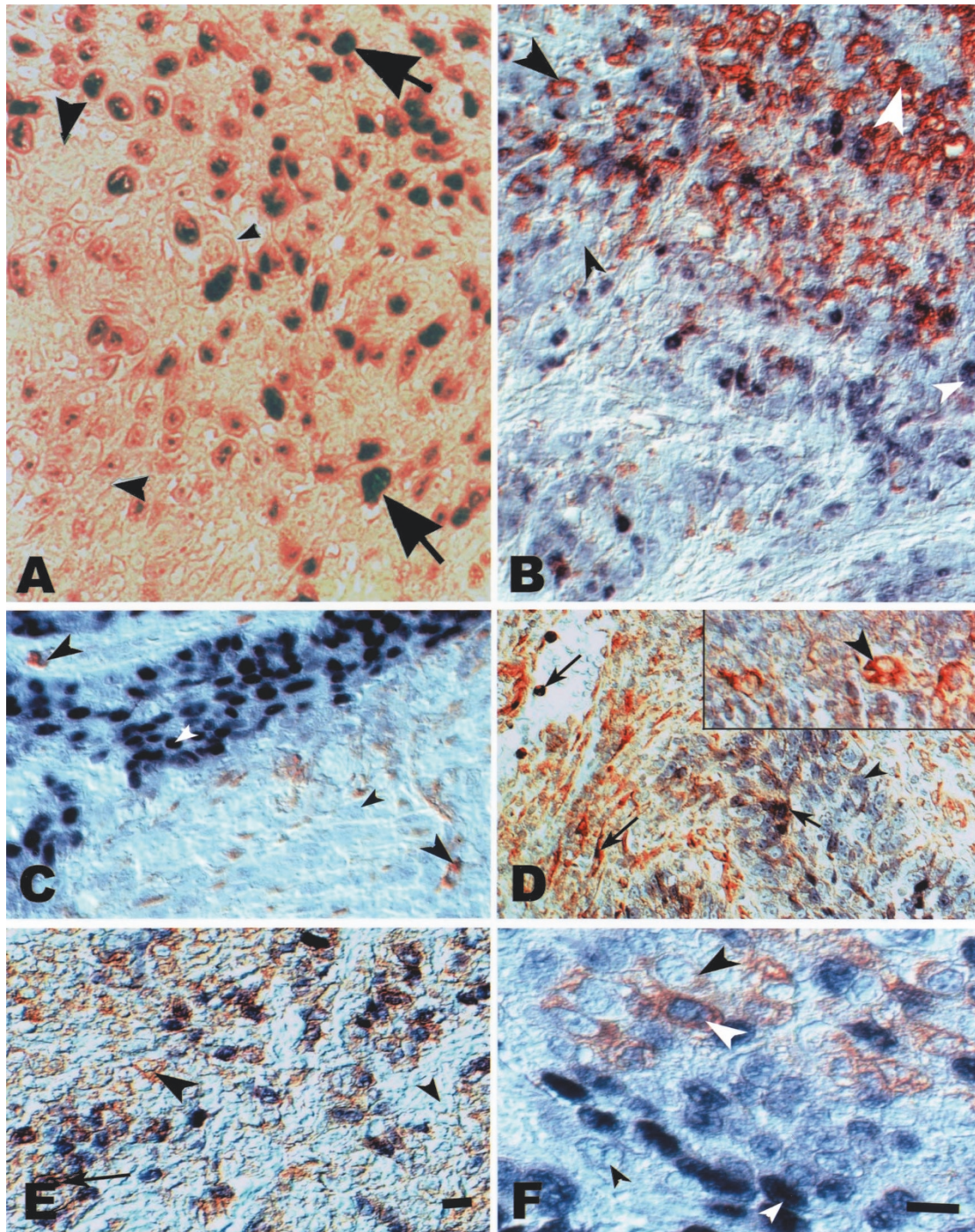

Figure 10.
Western blot analysis of epidermal growth factor receptor (EGFR) protein expression in EBV+ and EBV− NPC-TW04 cells. In the upper panel, the 170-kD band of EGFR is stronger in EBV+ cells than in EBV− cells. The densitometry analysis from gel electrophoresis in the lower panel indicates a 1.7-fold increase of EGFR in EBV+ cells.

grown faster and larger than EBV− tumors. In addition, in situ hybridization of EBER-1 and in situ PCR hybridization of BamH1 W fragments in NPC biopsy specimens all reveal clonal expansion of EBV+ tumor cells, which are surrounded by EBV− tumor cells. This indicates that EBV infection can accelerate NPC cell proliferation (Lin et al, 1994, 1997a). To support this hypothesis, we analyzed the function of EBV in NPC cells.

For in vitro investigation, we used the IgA receptor–mediated endocytosis method to infect NPC cells with EBV. Infection efficiency was 90% to 95% in three different cell lines and depended on degree of SC protein expression. Then, we used an MICS to examine degrees of cell invasion and migration after NPC cells had been infected with EBV for different time intervals. Our results (Fig. 2) indicate that EBV infection enhances NPC cell migration and invasion in vitro and that degree of invasion is time dependent. After 21 days, tumor cell invasion and migration decreased because many EBV genomes had been excreted through exocytosis. All EBV DNA became undetectable by PCR analysis 72 days after infection (Lin et al, 2000).

The mechanism of tumor cell invasion and migration enhancement was investigated by RT-PCR analysis of

Figure 11.

Localization of EBV genome by in situ PCR hybridization and co-localization of epidermal growth factor receptor (EGFR) + EBER-1, matrix metalloproteinase (MMP)-2 + EBER-1, MMP-9 + EBER-1, vascular endothelial growth factor (VEGF) + EBER-1 and basic fibroblast growth factor (bFGF) + EBER-1 in nasopharyngeal carcinoma (NPC) biopsy specimens. (A) The NPC biopsy section treated with in situ PCR hybridization of EBV *Bam*HI W fragment shows a fraction of EBV+ cells (*large arrows*) intermixed with EBV− cells (*large and medium arrowheads*). *Small arrowhead* indicates a keratinized tumor cell without EBV signal. (B) Co-localization of EGFR and EBER-1 in NPC biopsy specimen. Some EBV+ cells show strong EGFR immunoreactivity (*large white arrowhead*), but other EBV+ cells show no EGFR immunoreactivity (*small white arrowhead*). Some cells are strongly EGFR reactive without EBV signal (*large black arrowhead*). Others have neither EBER-1 nor EGFR staining (*small black arrowhead*). (C) Many EBV+ cells (*white arrowhead*) are distributed in a geographic pattern (MMP-2 + EBER-1). Other tumor cells are EBV− (*small black arrowhead*). No or very rare tumor cells contain both EBV signal and MMP-2 reaction product in this section. Only a few of EBV− cells also show MMP-2 reaction product (*large black arrowheads*). However, some interstitial cells also contain MMP-2 reaction product. (D) For MMP-9 + EBER-1, the reaction product of anti-MMP-9 (yellowish brown color) is seen in the cytoplasm of certain EBV− tumor cells (*large arrowhead* in the inset), and in some EBV+ tumor cells (*short arrow*). Some EBV+ cells are not MMP-9 immunoreactive (*small black arrowhead*). Some interstitial fibroblasts (*long arrow*) and mononuclear cells (*long arrow*) in the stromal region were also stained with anti-MMP-9 reaction product. (E) For VEGF + EBER-1, immunoreactivity of VEGF is seen in the cytoplasm of EBV+ (*arrow*) and EBV− (*large black arrowhead*) tumor cells. However, some tumor cells (*small black arrowhead*) reveal neither EBER-1 signal nor VEGF staining. Other tumor cells show EBV signal without VEGF immunoreactivity. (F) For bFGF + EBER-1, immunoreactivity of bFGF is seen in the cytoplasms of EBV+ (*large white arrowhead*) and EBV− (*large black arrowhead*) tumor cells. Some cells contain EBER-1 signal (purple, *small white arrowhead*) only. In addition, other tumor cells contain neither EBER-1 nor bFGF (*small black arrowhead*). Bar in E for A, B, C, D, and E = 40 μm; bar in F = 10 μm.

invasion-related host gene expressions. Both RT-PCR data (Fig. 3) and densitometry analysis (Fig. 4) suggest that MMP-2, MMP-9, and heparanase gene expressions are moderately up-regulated, that VEGF is mildly up-regulated, and that all are time dependent with some variation. The fact that these four RNA gene expressions were still up-regulated 3 weeks after EBV infection indicates that their mRNA may have a longer half-life, similar to that of GM-CSF gene expression, which was also up-regulated 3 weeks after infection, as shown in our previous report (Lin et al, 2000). In that study, we demonstrated that growth factor and cytokine genes, such as *EGFR*, *TGF-α*, *IL-1*, and *IL-6*, were up-regulated at 2 and 3 weeks and were decreased after 4 weeks of EBV infection, at which time a fraction of infected cells still contained copies of EBV genome. No EBV genome can be detected after 72 days. Although we did not include a 4-week incubation in the present experiment, we believe that mRNA expression of EGFR, heparanase, MMP-2, and MMP-9 would decrease after 4 weeks because of EBV genome excretion. These data suggest that EBV may not directly regulate these genes. It is likely that EBV proteins enhance these host gene expressions indirectly. There was no significant elevation of bFGF gene expression.

For in vivo investigation of EBV function in infected NPC cells, we established an animal model. In this model, we demonstrated that EBV+ tumors grew faster and larger than EBV− ones (Table 2). This finding suggests that EBV accelerates NPC tumor growth in vivo in SCID mice and differs from the hypothesis that EBV may be involved in initiation or early promotion of NPC tumorigenesis (Pathmanathan et al, 1995; Raab-Traub and Flynn, 1986). The argument that EBV initiates and promotes NPC tumorigenesis is based on molecular and morphologic findings from NPC patients and biopsy specimens, which can be summarized as follows: (a) Many NPC biopsy specimens contain the EBV genome with a clonal terminal repeat pattern (Raab-Traub and Flynn, 1986), and (b) Many NPC patients have high titers of IgA for EBV-VCA and other antigens. It was deduced that EBV infects and transforms nasopharyngeal squamous metaplastic epithelial cells. During clonal proliferation of transformed epithelial cells, EBV episomal plasmids replicate and produce the EBV genome with a clonal terminal repeat pattern. It was concluded that EBV participates in early carcinogenesis of NPC (Pathmanathan et al, 1995; Raab-Traub and Flynn, 1986).

However, our animal experiment and observations from NPC biopsy specimens do not support this conclusion; rather, they indicate that EBV plays another role by regulating enhancement of NPC tumor growth. This conclusion is based on the observation that analysis of EBV terminal repeat sequences in EBV+ tumors demonstrated that all tumors had a clonal (single band) EBV terminal repeat sequence that differed in size if different cell lines were examined. This finding goes against the hypothesis that a clonal EBV terminal repeat sequence can only be observed in a single epithelial cell transformed by EBV, thereby

resulting in clonal proliferation of tumor cells (Raab-Traub and Flynn, 1986).

This hypothesis is also not supported by our previous in vitro study that demonstrated a clonal EBV terminal repeat sequence in NPC cells infected by an EBV-IgA-SC complex (Lin et al, 1997b). It is apparent that epithelial NPC tumor cells infected in vivo by multiple EBV particles can also have a clonal EBV terminal repeat sequence. Therefore, we feel that a clonal EBV terminal repeat sequence does not fully explain NPC tumorigenesis. It should be pointed out that although single bands in lanes 3 and 4 (Fig. 6) could be explained by a single integration event after loss of all episomes, we feel such an event is unlikely.

In a previous experiment (Lin et al, 1997b; Fig. 4), we collected the total DNA from EBV+ NPC cells. It was digested by BamH1 endonuclease and hybridized by *Xho*I 1.9 kb and LMP2B probes. Results yielded EBV genomes of the same size, a finding that indicates EBV+ NPC cells contain an episomal form of the viral genome. Because this result has been published, we have not included the data in the present study. Our previous data have also shown that when EBV particles isolated from the B95–8 cell line were used to immortalize normal human peripheral lymphocytes, Southern blot analysis of EBV DNA in these lymphocytes demonstrated a polyclonal terminal repeat sequence with one major 15- to 20-kb band (Lin et al, 1997b). In the present experiment, we also performed Southern blot analysis of B95–8 cell line DNA and found multiple bands plus one major 18- to 30-kb band. The size of this major band is probably due to fusion of different termini and to the shorter gel electrophoresis time. Both methods show the same polyclonal EBV termini sequences. These results can be explained on the basis of differences in EBV particle behavior in different cell types. When EBV particles infect B lymphocytes, the linear form of EBV DNA fuses randomly to form the circular form. When EBV particles infect epithelial tumor cells, they may fuse randomly at first to form the circular form; within a short period of time, some cells that contain a specific size of circular form may proliferate faster than the cells that contain other circular form, resulting in the presence of a same size of circular form in the majority of infected cells; on the other hand, all infected linear forms may fuse at a same specific site in the epithelial cells. Under these circumstances, EBV genomes produced in B lymphocytes form polyclonal DNA sequences, while those produced in epithelial tumor cells form clonal DNA sequences. However, further experiment is needed to prove it.

EBV enhancement of NPC tumor growth in vivo may be due to the fact that EGFR, TGF-α, and unidentified growth factors are up-regulated in EBV+ cells. This is shown in the present animal experiment using RT-PCR and in a previous study in which in vitro EBV infection of NPC cells demonstrated up-regulation of EGFR and TGF-α (Lin et al, 2000). Previously, Miller et al (Miller et al, 1995) reported that EBV-LMP-1 protein induced EGFR expression in a uterine cervical cancer cell line that had been transfected with a plasmid

containing the LMP-1 DNA sequence. However, in the present experiment, average numbers of EBV+ and EBV− tumor cells that expressed EGFR in solid tumor sections were similar: 73 and 75, respectively. Immunostaining of EGFR was much stronger in EBV+ than in EBV− sections. This finding was supported by Western blot analysis of EGFR expression in EBV+ and EBV− cells, which showed that EBV+ cells had 1.7-fold increase in EGFR protein (Fig. 10).

It is possible that in the present animal experiment (although some NPC cells already expressed EGFR mRNA and protein), LMP-1 produced from EBV+ cells could also up-regulate the expressed *EGFR* gene. In those cells that did not express EGFR in EBV− tumor masses, EBV infection could not cause expression of the unexpressed *EGFR* gene (Fig. 8, A and B). The results from EGFR expression in the EBV+ and EBV− tumor cells in the in vitro and in vivo animal model and in the biopsy specimens (Fig. 11B) all suggest that EBV up-regulates EGFR only in cells that express EGFR, but not in cells that do not express EGFR. Because the present experiments were not designed to prove this assumption, this hypothesis needs further study. Although we feel that EBV enhances NPC progression, our experiment does not rule out a role for EBV in the initiation and promotion of NPC carcinogenesis. The finding that many biopsy specimen tumor cells that expressed strong EGFR were not infected by EBV (Fig. 11B) indicates that EGFR expression may be up-regulated both by EBV infection and by other unidentified factors.

The distribution of EBV-containing NPC cells (clonal proliferation) in sections of solid tumor (Fig. 5B) suggests that EBV+ cells grow faster than EBV− cells. It should be pointed out that cells derived from a mother cancer cell are genetically unstable and have different genotypes and phenotypes with variable growth characteristics. Therefore, EBV infection of tumor cells variably affects growth patterns. EBV up-regulates EGFR and TGF-α gene expression but not TGF-β and its receptor gene. Thus, only a subset of EBV+ cells may grow faster than other infected cells. Alteration of other growth factor genes in EBV− tumor cells could enhance their proliferation as well. If these cells were later infected by EBV, marked enhancement of tumor growth by up-regulated expression of other growth factor related genes could occur.

Because increased expression of matrix proteinases and angiogenic factors is needed for tumor invasion and proliferation, we evaluated EBV tumor growth promotion by studying two proteases associated with EBV infection: MMP-2 and MMP-9 (Horikawa et al, 2000; Takeshita et al, 1999; Yoshizaki et al, 1998). We also studied VEGF and bFGF because they are well known factors in angiogenesis. The moderate elevation and time-dependent expression of MMP-2 mRNA demonstrated by RT-PCR analysis indicate that EBV up-regulates MMP-2 expression. This finding is supported by double-localization data in tumor sections from SCID mice (Fig. 8, C and D). However, it should be pointed out that background staining presented difficulties in differentiating MMP-

2–positive cells from MMP-2–negative cells (Fig. 8C) Therefore, only those tumor cells with clear immunostaining were considered MMP-2 positive. Furthermore, the strongly positive reaction of stromal mesenchymal cells suggests that EBV induces host cell transcription of unidentified growth factors and cytokines, which up-regulate MMP-2 gene expression, probably through a paracrine effect. Results from NPC biopsy specimens demonstrated that some EBV+ cells did not express MMP-2, an indication that EBV cannot activate the unexpressed *MMP-2* gene in host cells (Fig. 10C).

In the case of MMP-9, EBV up-regulated MMP-9 expression in in vitro EBV+ cells and in in vivo EBV+ solid tumors. Furthermore, in the NPC biopsy specimens, MMP-9 protein expression was increased in stromal mesenchymal cells. The strong MMP-9 expression in these cells may not be related to EBV infection. It is possible that NPC cells secrete growth factors and cytokines that stimulate stromal cells. The fact that some EBV+ cells in NPC biopsy specimens contained no MMP-9 protein (Fig. 11D) suggests that EBV does not activate the unexpressed *MMP-9* gene. The fact that some EBV− tumor cells were MMP-9 positive indicates that MMP-9 expression is regulated by other factors.

Recently, Takeshita et al (Takeshita et al, 1999) have demonstrated up-regulation of endogenous MMP-9 gene expression and exogenous MMP-9 promoter activity in a uterine cervical cancer cell line transfected by wild-type LMP-1. They concluded that activation of NF-kB and AP-1 pathways by LMP-1 is necessary for activation of MMP-9 expression. We found that certain NPC cells in both xenograft tissue sections and NPC biopsy specimens showed up-regulated MMP-9 expression in cells infected by EBV. Our data support the findings of Takeshita et al (Takeshita et al, 1999). Because our study showed EBV+ tumor cells in xenograft and NPC biopsy specimens without MMP-9 expression (Figs. 8 and 10), the results of a transfection experiment on a cell line without MMP-9 expression would be pertinent to our research.

Based on findings from in vitro RT-PCR analysis of EBV+ cells (Figs. 3C and 4), in vivo EBV+ SCID mouse tumor sections (Figs. 9, A and B) and NPC biopsy specimens (Fig. 11E), we propose that EBV regulates VEGF gene expression. However, because some EBV+ cells did not express VEGF, we also suggest that EBV does not activate the unexpressed VEGF gene. Since RT-PCR analysis showed no significant differences in bFGF expression in EBV+ and EBV− cells, we believe EBV has little or no role in the regulation of bFGF expression (Figs. 3D, 4, and 11F). Recently, Vlodavsky et al (Vlodavsky et al, 1999) have proposed that heparanase is an important protease involved in tumor invasion. In our RT-PCR analysis of heparanase expression in EBV+ and EBV− cells, we found that EBV infection moderately up-regulated heparanase expression (Figs. 3E and 4). We suggest that heparanase enhances NPC cell invasion. This proposal needs further investigation.

In conclusion, EBV enhances NPC cell proliferation, invasion, and tumor growth by up-regulating EGFR, TGF-α, MMP-2, MMP-9, VEGF, and other unidentified genes in cells that express those genes. However, EBV does not up-regulate EGFR, MMP-2, MMP-9, VEGF, and bFGF in cells that do not express these genes. Although we feel that EBV enhances NPC progression, our experiment does not rule out a role for EBV in the induction and promotion of NPC development. Furthermore, unidentified factors may enhance NPC proliferation independent of EBV infection.

Materials and Methods

Cell Lines and Culture

In this experiment, we used two representative NPC cell lines established in our laboratory (NPC-TW01 and 06). NPC-TW01 (Lin et al, 1990) was derived from a 64-year-old male NPC patient with keratinizing squamous cell carcinoma (WHO Type I) and NPC-TW 06 (Lin et al, 1993) were derived from a 58-year-old female NPC patient with an undifferentiated carcinoma (WHO Type IIb). Although the lines contained EBV DNA at early passages, they became negative after 30 passages (Lin et al, 1994).

EBV Infection of NPC Cells

EBV particles isolated from a B95–8 cell line were used to infect NPC cells according to the method of receptor mediated endocytosis as previously described (Lin et al, 1997a; Sixbey and Yao,1992). Briefly, NPC-TW01 (WHO Type I) and NPC-TW04 and 06 (WHO Type IIb) cells were incubated with diluted (1:50 dilution) NPC patient serum containing high titer (1:640) of IgA anti-EBV-VCA at 4° C, separately, for 30 minutes. After washing, EBV particles were added, and the cells were re-incubated for another 30 minutes at 4° C, and then transferred to a CO_2 incubator, incubated at 37° C for 30 minutes. Finally, the regular culture medium (DMEM + 5% FCS) was used, and the cells were cultured for 21 days. Some tumor cells were collected on Day 7, 10, 14, and 21 and subjected to in vitro invasion assay (Chu et al,1993), semi-quantitative RT-PCR analysis (Lin et al, 2000); and others were checked by PCR Southern blotting and in situ PCR hybridization (Lin et al, 1994) to make sure that the infection process was complete. To be sure that NPC cells could only be infected by IgA anti-EBV-VCA + EBV particles, we further divided the NPC cells into two groups: one group was treated with high titer of NPC antiserum IgA anti-EBV-VCA and EBV particle as mentioned above, and the other group was treated with EBV only. Both groups were further incubated for 7 days. Then part of each group was fixed for in situ PCR hybridization; another part of each group was fixed for immunostaining using mAb against EBNA-1 as we have done previously (Lin et al, 2000).

Tumor Invasion Assay

To investigate the NPC cell invasion ability, we used MICS (Chu et al, 1993; Hendrix et al, 1987). It is a multifaceted system to examine a number of steps involved in cell invasion and migration. We used 10-μm pore size of a nitrocellulose membrane coated with a mixture of 5 mg/ml matrigel, applied 2.5×10^4 NPC-TW01 cells after EBV infection for 0, 7, 14, and 21 days, separately, and incubated in DMEM containing 10% Nuserum for 48 hours. The invaded cells were then fixed and stained with propidium iodide and counted with computer software under a magnification of $\times 50$. The experiments were repeated three times.

Semi-Quantitative RT-PCR Analysis of Gene Expressions Related to Tumor Invasive Proteases and Angiogenic Factors in EBV-Infected NPC Cells

We selected MMP-2, MMP-9, and heparanase as representative matrix proteases, and used VEGF and bFGF as representative angiogenic factors to investigate their gene expressions in EBV-infected NPC cells. The procedure of RT-PCR, including the isolation of total RNA, reverse transcription, and PCR analysis, was performed according to our previous publication (Lin et al, 2000). The primers we used are shown in Table 1. Two pairs of actin primer sequences (one includes 318 bp and the other 173 bp) were used for internal control. The sequences were exactly similar to our previous publication (Lin et al, 2000). The results from gel analysis of RT-PCR were further analyzed by densitometry.

Establishment of the SCID Mouse Model Bearing with EBV-Infected NPC Tumors

EBV-free NPC cells (1×10^7 cells per mouse) were injected into 10 SCID mice subcutaneously. Seven days later, the tumor masses (about 0.5 cm in diameter) in each of five mice were injected directly with IgA-anti-EBV-VCA (0.2 ml of $\times 50$ diluted NPC patient serum) and 0.2 ml of $\times 100$ concentrated EBV solution (EBV solution was obtained from $\times 100$ concentrated B95–8 cell culture medium), separately. After another 21 days, the tumor masses were removed, measured, and dissected into several pieces and randomly subjected to identification of EBV genome and tumor gene expressions. In each of another two mice, the tumors were injected with EBV only without IgA as the EBV-free control group. In another three mice, each tumor mass did not injected with any substance, as a negative control.

For identification of EBV genome in the solid tumor masses removed from the SCID mice, total DNAs from each mass were isolated by SDS lysis, proteinase K digestion, and phenol-chloroform extraction and subjected to PCR and Southern blotting using BamH1 W fragment of EBV genomic DNA (Lin et al, 1994) as the probe. We also applied in situ PCR hybridization (Lin et al, 1994, 1997a) using a two-step method. The first step was to perform in situ PCR (the PCR primers were designed from BamH1 W fragment). The second step was to perform in situ hybridization (using the DNA fragment as the probe, which was derived from the inner region of two primers in BamH1 W fragment

and labeled with digoxigenin) to localize EBV genome in the tumor sections, and in situ hybridization using the EBER-1 (EBV encoded small nuclear RNA-1) anti-sense probe to detect the EBV small nuclear RNA (Lin et al, 1994) to see whether the infected EBV could still transcript its mRNA. For identification of the EBV terminal repeat sequences in the solid tumor mass, we used *Bam*HI endonuclease to digest DNA, and subjected it to Southern blotting using the *Xho*I 1.9 kb in the right terminus region of EBV genome as the probe (Lin et al, 1997b; Raab-Traub and Flynn, 1986).

Identification of Changes in Gene Expressions in EBV-Infected NPC Tumors from SCID Mice by RT-PCR

Semi-quantitative RT-PCR analysis (Ausubel et al, 1988; Lin et al, 2000) was used to detect the changes in mRNA expressions of growth factor genes and one *SC protein* gene. These included EGFR, TGF-α, TGF-β, TGFβR-I, TGFβR-II, and *SC protein* genes. Total RNAs were extracted from EBV-infected and EBV-free solid tumor masses (Lin et al, 1994) and subjected to reverse transcription. The cDNAs were used as the template for a touch-down PCR program (Lin et al, 2000). The final PCR reaction product was analyzed by gel electrophoresis. In each experiment, a pair of actin or glyceraldehyde phosphate dehydrogenase primers as the internal control was included. The sequence of PCR primers was exactly similar to our previous publication (Lin et al, 2000).

Western Blot Analysis of EGFR Expression in EBV-Infected and EBV-Free NPC Cells

After NPC-TW04 cells were infected by EBV as mentioned above for 7 days, the total protein was extracted from the same numbers of EBV-infected and EBV-free NPC cell pellets by direct mixing with denature sample buffer and subjected to 10% SDS-polyacrylamide gel electrophoresis. Routine Western blotting (Lin et al, 1993) was performed using antibodies against EGFR or tublin for internal control.

Double-Localization of Growth Factors and Tumor Invasion Factors in EBV-Infected and EBV-Free Solid Tumors Obtained from SCID Mice and NPC Biopsy Specimens

The procedure for double-localization of protein and EBER-1 was performed according to our previously published method (Lin et al, 1997a). Briefly, the tumor masses obtained from the SCID mice were fixed in 3% formaldehyde, dehydrated, and embedded in paraffin blocks. The paraffin sections, after deparaffinization, were preheated or not and then first incubated with antibodies against EGFR, MMP-2, MMP-9, VEGF, and bFGF, separately, followed by biotinylated second antibodies and avidin-biotin peroxidase complex, and finely subjected to peroxidase substrate treatment according to the routine method. The sections were further subjected to in situ hybridization of EBER-1 according to our previously published procedure (Lin et al, 1997a).

For double-localization in biopsy specimens, 20 NPC biopsy paraffin blocks were collected from the recent surgical biopsy file from the Department of Pathology at National Taiwan University Hospital. Eighteen cases were WHO Type IIb undifferentiated NPC, and two cases were WHO Type I keratinizing squamous cell NPC. The male to female ratio was 3:1. The range of age was between 35 to 55 years old. All were the primary biopsy specimens. Seventy percent of these patients showed neck lymph node metastasis only. The most common clinical symptoms included neck lymph node enlargement, nasal obstruction, nasal bleeding, one side tinnitus, bloody sputum, one-side facial nerve impairment and one-side headache. All specimens were subjected to EBER-1 in situ hybridization and in situ PCR hybridization using the method previously described (Lin et al, 1994; Lin et al, 1997a). In addition, some of them (two to three cases) were subjected to co-localization of EGFR, MMP-2, MMP-9, VEGF, and bFGF, with EBER-1, separately.

References

Armstrong RW, Armstrong MJ, Yu CM, and Henderson BE (1983). Salted fish and inhalants as risk factor for nasopharyngeal carcinoma in Malaysian Chinese. Cancer Res 43: 2967–2970.

Ausubel FM, Brent R, Kingston RE, Moore DD, Seidman JG, Smith JA, and Struhl K, editors (1988). Current protocols in molecular biology. New York: Green Publishing Associates and Wiley-Interscience.

Chu YW, Runyan RB, Oshima RG, and Hendrix MJC (1993). Expression of complete keratin filaments in mouse L cells augments cell migration and invasion. Proc Natl Acad Sci USA 90:4261–4265.

Hendrix MJC, Seftor EA, Seftor REV, and Fidler IJ (1987). A simple quantitative assay for studying the invasive potential of high and low metastatic variants. Cancer Lett 38:137–147.

Ho CK, Lo WCH, Huang PH, Wu MT, Christiani DC, and Lin CT (1999). Suspected nasopharyngeal carcinoma in three workers with long-term exposure to sulfuric acid vapor. Occup Environ Med 56:426–428.

Horikawa T, Yoshizak T, Sheen TS, Lee SY, and Furukawa M (2000). Association of latent membrane protein 1 and matrix metalloproteinase 9 with metastasis in nasopharyngeal carcinoma. Cancer 89:715–723.

Klein G, Giovanella BC, Lindahl T, Fialkow RJ, Singh S, and Stehlin JS (1974). Direct evidence for the presence of Epstein-Barr virus DNA and nuclear antigen in malignant epithelial cells from patients with poorly differentiated carcinoma of the nasopharynx. Proc Natl Acad Sci USA 71:4737–4741.

Lin CT, Chan WY, Chen W, Huang HM, Wu HC, Hsu MM, and Chuang SM (1993). Characterization of seven newly estab-

lished nasopharyngeal carcinoma cell lines. Lab Invest 68: 716–727.

Lin CT, Chen W, Hsu MM, and Dee AN (1997b). Clonal versus polyclonal Epstein-Barr virus infection in nasopharyngeal carcinoma cell lines. Lab Invest 76:793–798.

Lin CT, Dee AN, Chen W, and Chan WY (1994). Association of Epstein-Barr virus, human papilloma virus and human cytomegalovirus in nine nasopharyngeal carcinoma cell lines. Lab Invest 71:731–736.

Lin CT, Kao HJ, Lin JL, Chan CY, Wu HC, and Liang ST (2000). Response of nasopharyngeal carcinoma cells to Epstein-Barr virus infection in intro. Lab Invest 80:1149–1160.

Lin CT, Lin CR, Tan GK, Chen W, Dee AN, and Chan WY (1997a). The mechanism of Epstein-Barr virus infection in nasopharyngeal carcinoma cells. Am J Pathol 150:1745–1756.

Lin CT, Wong CI, Chan WY, Tzung KW, Ho JKC, Hsu MM, and Chuang SM (1990). Establishment and characterization of two nasopharyngeal carcinoma cell lines. Lab Invest 62:713–724.

Miller WE, Earp HS, and Raab-Traub N (1995). The Epstein-Barr virus latent membrane protein 1 induces expression of the epidermal growth factor receptor. J Virol 69:4390–4398.

Morgan M, Kniss D, and McDonnell S (1998). Expression of metalloproteinases and their inhibitors in human trophoblast continuous cell lines. Expt Cell Res 242:18–26.

Niedobitek G, Hansmann ML, Herbst H, Young LS, Dienemann D, Hartmann CA, Finn T, Pitteroff S, Welt A, Anagnostopoulos I, Friedrick R, Lobeck H, Sam CK, Araujo I, Rickinson AB, and Stein H (1991). Epstein-Barr virus and carcinoma: Undifferentiated carcinoma but not squamous cell carcinomas of the nasopharynx are regularly associated with the virus. J Pathol 165:17–24.

Nuovo GJ, MacConnell PB, Simsir A, Valea F, and French DL (1995). Correlation of the in situ detection of polymerase chain reaction-amplified metalloproteinase complementary DNAs and their inhibitors with prognosis in cervical carcinoma. Cancer Res 55:267–275.

Ohta Y, Endo Y, Tanaka M, Shimizu J, Oda M, Hayashi Y, Watanabe Y, and Sasaki T (1996). Significance of vascular endothelial growth factor messenger RNA expression in primary lung cancer. Clin Cancer Res 2:1411–1416.

Pathmanathan R, Prasad U, Salder R, Flynn K, and Raab-Traub N (1995). Clonal proliferations of cells infected with Epstein-Barr virus in preinvasive lesions related to nasopharyngeal carcinoma. N Engl J Med 333:693–698.

Raab-Traub N and Flynn D (1986). The structure of the termini of the Epstein-Barr virus as a marker of clonal cellular proliferation. Cell 47:883–889.

Raab-Traub N, Hood R, Yang CS, Henry BI, and Pagano JS (1983). Epstein-Barr virus transcription in nasopharyngeal carcinoma. J Virol 48:580–590.

Sixbey JW and Yao QY (1992). Immunoglobulin A-induced shift of Epstein-Barr virus tissue tropism. Science 225:1578–1580.

Takeshita H, Yoshizaki T, Miller W, Sato H, Furukawa M, Pagano JS, and Raab-Trau BN (1999). Matrix metalloproteinase 9 expression is induced by Epstein-Barr virus latent membrane protein 1 C-terminal activation regions 1 and 2. J Virol 73:5548–5555.

Vlodavsky I, Friedmann Y, Elkin M, Aingorn H, Atzmon R, Ishai-Michaeli R, Bitan M, Pappo O, Peretz T, Michal I, Spector L, and Pecker I (1999). Mammalian heparanase: Gene cloning, expression and function in tumor progression and metastasis. Nat Med 5:793–802.

Waterhouse L, Muir C, Shanmugaratnam K, Powell J, Peacham D, and Whelan S (1982). Cancer Incidence in Five Continents, International Agency for Research on Cancer Scientific Publication 42, vol 4. Lyon: International Agency for Research on Cancer.

Yoshizaki T, Sata H, Furukaka M, and Pagano JS (1998). The expression of matrix metalloproteinase 9 is enhanced by Epstein-Barr virus latent membrane protein 1. Proc Natl Acad Sci USA 95:3621–3626.